Complex unstable periodic orbits and their manifestation in classical and quantum dynamics

G. Contopoulos,[1] S. C. Farantos,[2,*] H. Papadaki,[1] and C. Polymilis[1]
[1]*Department of Astronomy, University of Athens, Panepistimiopolis, Athens, Greece*
[2]*Department of Chemistry, University of Crete, and Institute of Electronic Structure and Laser, Foundation for Research and Technology Hellas, Iraklion, Crete 711 10, Greece*
(Received 11 March 1994; revised manuscript received 3 August 1994)

A model system of three degrees of freedom which has a complex unstable family of periodic orbits is studied both classically and quantum mechanically. It is shown that the classical and quantum mechanical survival probability functions are in good agreement, and both functions reveal the characteristics of complex unstable periodic orbits, i.e., the exponential divergence with rotation of nearby trajectories.

PACS number(s): 05.45.+b, 03.65.−w, 03.20.+i

I. INTRODUCTION

The correspondence between classical and quantum mechanics, particularly in the regime of strong classical chaos, has been the subject of intense research for the last 20 years [1]. One of the main results of this work was the discovery of the importance of classical periodic orbits for a semiclassical approximation of the density of states, which was first proposed by Gutzwiller [2,3]. This work was later extended by Balian and Bloch [4], Berry and Tabor [5], and Miller [6]. An impetus was given by the study of the stadium model by McDonald and Kaufman [7] and particularly by Heller [8], who showed that the eigenfunctions of this chaotic model have increased amplitude along the unstable periodic orbits. These results have been supported by a large number of studies on model and real systems, such as the hydrogen atom in strong magnetic fields [9].

Most of these studies are for two degrees of freedom systems, and relatively little work has been done for three-dimensional (3D) dynamical systems. Three-dimensional systems show new dynamical phenomena, such as the *Arnold diffusion,* [10], i.e., the nonisolation of the chaotic regions in phase space, and the phenomenon of *complex instability* [11]. The latter is related to unstable periodic orbits whose monodromy matrix has a quadruplet of complex eigenvalues out of the unit circle. This can happen only for systems with three or more degrees of freedom. Around complex unstable periodic orbits the trajectories diverge exponentially while rotating with a characteristic frequency. The quantum mechanical counterpart of the classical complex instability has not been studied yet.

In this article, we investigate the correspondence between classical and quantum mechanics in the region of complex unstable periodic orbits. A 2D model, examined by us before [12], is extended into a 3D system, which shows complex instability. Specifically, the system which we employ is described by the Hamiltonian

$$H=\tfrac{1}{2}(p_x^2+p_y^2+p_z^2)+\tfrac{1}{2}(\omega_x^2x^2+\omega_y^2y^2+\omega_z^2z^2) -\epsilon x^2y-\eta x^2z\ . \quad (1)$$

The values of the parameters are $\omega_x^2=0.9$, $\omega_y^2=1.6$, $\omega_z^2=0.4$, $\epsilon=0.08$, and $\eta=0.01$. The harmonic frequencies satisfy the following resonance conditions: $\omega_x:\omega_y:\omega_z=3:4:2$. The Hamiltonian system of Eq. (1) has been studied extensively by one of us (G.C.) for several values of its parameters [13,14].

In our previous study of the 2D model ($z=0$), we systematically investigated the correspondence of the most important families of periodic orbits with the first 100 eigenfunctions. It was found that the family 1:2 (along the x and y axes) influences the eigenfunctions that have nodes along the x axis. This family remains stable for the energy range 0–21 energy units. The corresponding family in the 3D system is a 1:2:2 resonance. The parameter values which we have chosen for the 3D model turn this family of periodic orbits into complex unstable orbits from almost the bottom of the well ($E=0$) up to about 12 energy units. After this energy, the periodic orbit becomes stable. Figure 1 shows the (x,y) projection of this periodic orbit. Thus this family of periodic orbits serves

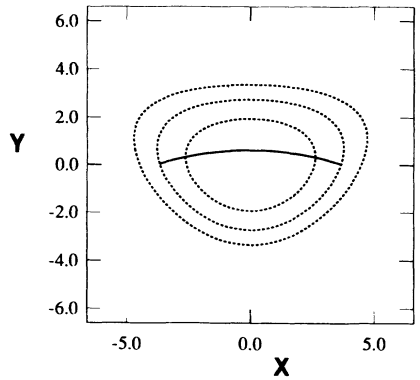

FIG. 1. Projection of a complex unstable periodic orbit in the (x,y) plane. Initial conditions $x,p_x,y,p_y,z,p_z=0.0$, 3.371 135 3, 0.623 059 6, 0.0, 0.189 221 2, 0.0, and $E=6$. The broken lines are contours of the potential function at energies 3, 6, and 9.

*Author to whom correspondence should be addressed.

as a model for investigating the phenomenon of complex instability in classical and quantum dynamics.

II. COMPLEX UNSTABLE PERIODIC ORBITS

The stability of a periodic orbit is examined by obtaining the eigenvalues of the monodromy matrix, i.e., by integrating the variational equations for one period with initial conditions equal the unit matrix. For a time independent Hamiltonian system the eigenvalues come in pairs of complex conjugate or inverse numbers, and two of them are equal to 1. Stable periodic orbits have all eigenvalues lying on the unit complex circle. Simply unstable periodic orbits have one pair of reciprocal real numbers, whereas doubly unstable periodic orbits have two pairs of real reciprocal numbers.

Complex unstable periodic orbits have a quadruplet of complex conjugate numbers with measures $|\lambda|$ and $1/|\lambda|$ different from 1, and thus can appear in systems of at least three degrees of freedom. In the linear approximation, the nearby trajectories will diverge or converge to the periodic orbit according to the law

$$\xi(t)=\xi(0)\exp(\pm\lambda t)\exp(\pm ivt)\ , \tag{2}$$

where t is a multiple of the period T, ξ is the vector of the differences in the coordinates and conjugate momenta of the two neighboring trajectories, λ is the Lyapunov exponent which dictates the rate of exponential divergence (convergence) from the periodic orbit, and v is the frequency of rotation of the neighboring trajectory around the periodic orbit. Equation (2) will be valid for a not very long time interval and for not large deviations from the periodic orbit (see Appendix).

In Table I we store the values of the Lyapunov exponent, rotational frequency, and period of the complex unstable periodic orbits for energies up to $E=12$. Comparison of the rotational frequency with the vibrational frequency along the periodic orbit ($\omega=0.948\,68$) reveals a ratio of about $v:\omega\approx 1:3$. This type of resonance condition should appear on a Poincaré surface of section.

Figure 2 shows a projection of a surface of section $x=0$, with total energy equal to 6 and on the plane (y,z). Figure 2(a) shows the early evolution of a nearby trajectory, and Fig. 2(b) shows the pattern of the surface of section for longer times. From these figures the spiral motion of the trajectory can be seen, as well as the restriction of the trajectory, in a certain region of phase space [Fig. 2(b)]. The appearance of the three branches of points in Fig. 2(a), plotted in a clockwise sense, is the result of the 1:3 approximate resonance condition. The points in Fig. 2(b) are concentrated along three wings and give a propellerlike shape to the pattern. A proof of the spiral motion of a nearby trajectory predicted by the variational equations, as well as a comparison with the numerical integration of the trajectory, is given in the Appendix. The question that we have addressed is, what happens in quantum mechanics, and this is the subject of the next section.

TABLE I. Lyapunov exponents, rotational frequencies, and periods of the complex unstable periodic orbit 1:2:2 at several energies.

Energy	λ	v	Period
2	0.002 586	0.310 31	6.665 94
3	0.003 934	0.307 04	6.687 18
4	0.005 270	0.303 54	6.708 26
5	0.006 551	0.299 80	6.729 13
6	0.007 725	0.295 80	6.749 78
7	0.008 725	0.291 54	6.770 17
8	0.009 462	0.286 98	6.790 27
9	0.009 810	0.282 13	6.810 06
10	0.009 561	0.276 95	6.829 51
11	0.008 294	0.271 41	6.848 59
12	0.004 516	0.265 49	6.867 29

III. CLASSICAL AND QUANTUM AUTOCORRELATION FUNCTIONS

To study the temporary behavior of an initial Gaussian wave packet centered at one point of the complex unstable periodic orbit we solve the time dependent Schrödinger equation numerically on a cubic grid with spectral methods. Specifically, we have used a fast

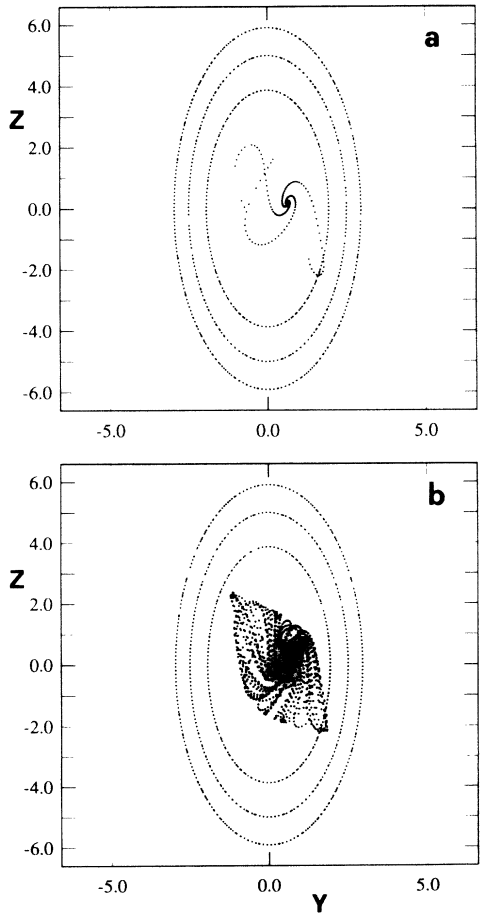

FIG. 2. Projection in the (y,z) plane of the Poincaré surface of section $(x=0)$ of a diverging trajectory from the complex unstable periodic orbit (a) for 600 periods and (b) for 2000 periods. Contours of the potential function are shown at 3, 5, and 7 units.

Fourier transform technique to evaluate the action of the Laplacian operator on the wave function, and a second order finite difference method to propagate the wave function in time [15]. The autocorrelation function is then computed as

$$C(t)=\int \phi(\mathbf{q},0)\exp\left[-\frac{i\mathcal{H}t}{\hbar}\right]\phi(\mathbf{q},0)d\mathbf{q}\ , \tag{3}$$

where $\phi(\mathbf{q},0)$ denotes the initial Gaussian wave packet, $\mathbf{q}=(x,y,z)$ and $\mathcal{H}$ is the Hamiltonian operator.

Figure 3 shows snapshots of the evolution of the wave packet initially localized on the periodic orbit that we examine. Notice that in this figure we plot $|\phi(t)|^2$ in the (y,z) plane after obtaining the intersection of the wave function with the plane $x=0$.

The classical analog of the quantum mechanical survival probability function $|C(t)|^2$ is given by [16–18]

$$\Omega(t)=\int \rho[\mathbf{q}(0),\mathbf{p}(0)]\rho[\mathbf{q}(t),\mathbf{p}(t)]d\mathbf{q}\,d\mathbf{p}\ . \tag{4}$$

$\rho[\mathbf{q}(0)]$ is an initial distribution of a batch of trajectories with initial conditions $\mathbf{q}(0)$. ρ is also a Gaussian distribution in phase space, and $\rho(t)$ is obtained by solving Hamilton's equations.

Figure 4 shows both the quantum (continuous line) and the classical (broken line) autocorrelation functions. The two curves almost coincide for the total integration time, about 25 periods of the periodic orbit, and in the inset of this figure we give a magnification of the last four peaks.

IV. DISCUSSION

The results of the previous section reveal the good agreement between classical and quantum mechanics. Comparing the snapshots of the wave packet in Fig. 3 with Fig. 2(b) we can see that the wave packet is restricted in the same region of the configuration space as the corresponding projection of the Poincaré surface of section. Figures 3(e)–3(h) also show that the high amplitude of the wave function occurs at the corners of the classical surface of section [Fig. 2(b)], which coincide with the turning points of the trajectory.

Comparison of the classical and quantum survival probability functions is even more revealing. The intensities of the lines, especially at the early stages of the evolution, demonstrate the 1:3 relation between the stability frequency (v) and the vibrational frequency ω along the periodic orbit. Particularly, examination of the classical autocorrelation function, computed for isolated trajectories close to the periodic orbit, demonstrates that at time $t=3nT$, $\Omega(t)$ takes larger values. The agreement between classical and quantum autocorrelation functions emphasizes the common dynamics present in both classical and quantum mechanics.

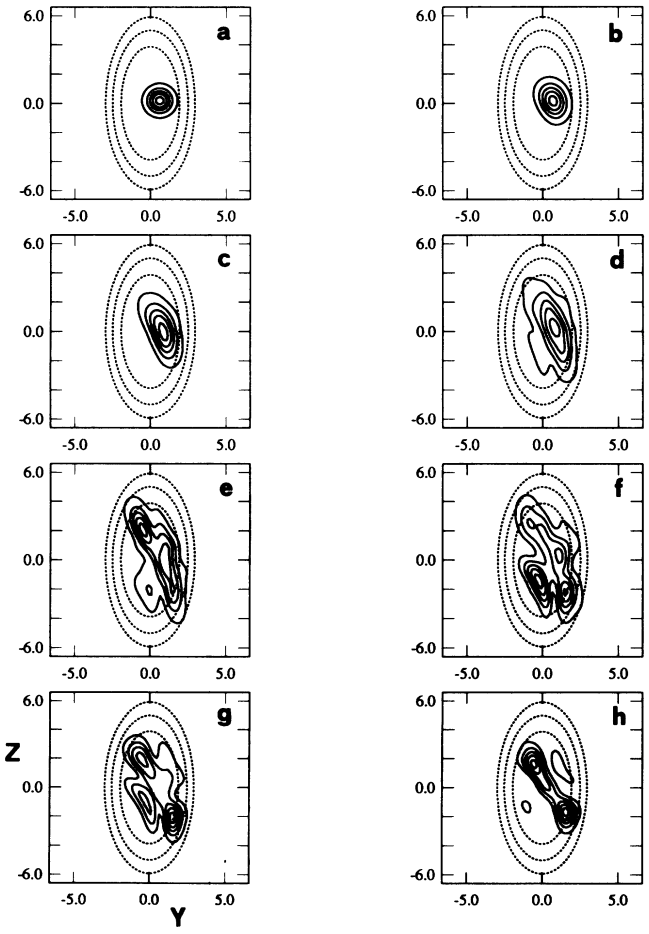

FIG. 3. Snapshots of the evolution of an initial Gaussian wave packet centered on the periodic orbit shown in Fig. 1. The frames correspond to the times (a) $t=0$, (b) 20.48, (c) 40.96, (d) 61.44, (e) 81.92, (f) 102.4, (g) 122.88, and (h) 143.36. The contours correspond to 10%, 30%, 50%, 70%, and 90% of the maximum amplitude. Contours of the potential function (broken lines) are also shown at 3, 5, and 7 energy units.

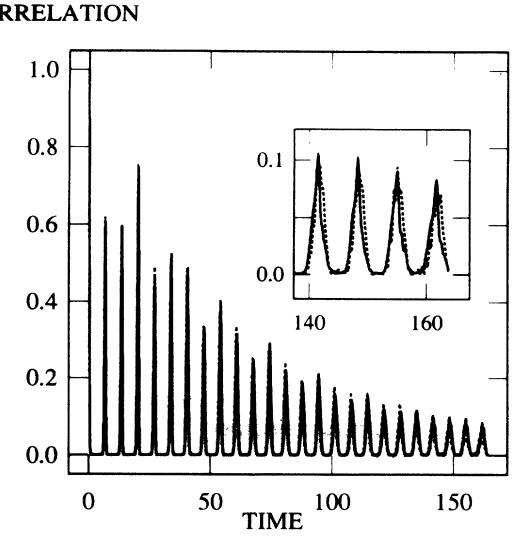

FIG. 4. Square of the quantum mechanical autocorrelation function (continuous line) and its classical mechanical analog (broken line).

Heller [19] has extensively studied the correspondence between classical and quantum survival probability functions for 2D dynamical systems. For unstable periodic orbits he argued that

$$|C(t)|^2 \approx \exp(-\lambda t) . \tag{5}$$

We have shown that in the case of complex unstable periodic orbits in a 3D system the survival probability function shows an exponential decay, but with a modulation in the amplitude of the lines dictated by the stability frequency.

Such a pattern of the quantum autocorrelation function, which is an observable quantity, leads one to look for manifestations of complex instability in physical systems. We have computed the eigenfunctions characterized by the periodic orbit 1:2:2, by Fourier transforming the wave packet, using the eigenenergies obtained also by a Fourier transform of the correlation function. We found that these eigenfunctions are of the type $(n,0,0)$, where n is the quantum number denoting levels having their nodes along the x axis. In other words, these complex unstable periodic orbits mark eigenfunctions of the system, as was found for two degrees of freedom systems both for stable and unstable periodic orbits. The study of molecular type potentials has shown that complex instability may be observed in molecules such as HCN [20], where it was found that periodic orbits of the rotating type turn from doubly unstable to complex unstable, and also in acetylene [21].

Summarizing our results, we have shown that the main characteristics of complex unstable periodic orbits, and particularly the exponential divergence with a simultaneous rotation of nearby trajectories, are reflected both in the classical and quantum survival probability functions.

ACKNOWLEDGMENT

We are glad to acknowledge financial support from the General Secretariat for Research and Technology (Grant No. PENED 89EΔ86).

APPENDIX

For a complex unstable periodic orbit of period T the eigenvalues are given by the equations

$$\begin{aligned} \mu_{1,2} &= e^{\lambda T}(\cos\theta \pm i \sin\theta) , \\ \mu_{3,4} &= e^{-\lambda T}(\cos\theta \pm i \sin\theta) , \end{aligned} \tag{A1}$$

where $e^{\lambda T} > 1$ and $0 < \theta < \pi$.

The corresponding eigenvectors are

$$\begin{aligned} \mathbf{z}_{1,2} &= \mathbf{x}_0 \pm i\mathbf{y}_0 , \\ \mathbf{z}_{3,4} &= \mathbf{u}_0 \pm i\mathbf{w}_0 . \end{aligned} \tag{A2}$$

After n periods T the above equations become

$$\begin{aligned} \mathbf{z}_{1,2}(nT) = e^{n\lambda T}\{&[\cos(n\theta)\mathbf{x}_0 - \sin(n\theta)\mathbf{y}_0] \\ &\pm i[\sin(n\theta)\mathbf{x}_0 + \cos(n\theta)\mathbf{y}_0]\} , \\ \mathbf{z}_{3,4}(nT) = e^{-n\lambda T}\{&[\cos(n\theta)\mathbf{u}_0 - \sin(n\theta)\mathbf{w}_0] \\ &\pm i[\sin(n\theta)\mathbf{u}_0 + \cos(n\theta)\mathbf{w}_0]\} . \end{aligned} \tag{A3}$$

Orbits with initial conditions $\mathbf{x}_0, \mathbf{y}_0, \mathbf{u}_0, \mathbf{w}_0$ after n periods are, respectively,

$$\begin{aligned} \mathbf{x}(nT) &= e^{n\lambda T}[\cos(n\theta)\mathbf{x}_0 - \sin(n\theta)\mathbf{y}_0] , \\ \mathbf{y}(nT) &= e^{n\lambda T}[\sin(n\theta)\mathbf{x}_0 + \cos(n\theta)\mathbf{y}_0] , \\ \mathbf{u}(nT) &= e^{-n\lambda T}[\cos(n\theta)\mathbf{u}_0 - \sin(n\theta)\mathbf{w}_0] , \\ \mathbf{w}(nT) &= e^{-n\lambda T}[\sin(n\theta)\mathbf{u}_0 + \cos(n\theta)\mathbf{w}_0] . \end{aligned} \tag{A4}$$

Thus an orbit with initial conditions

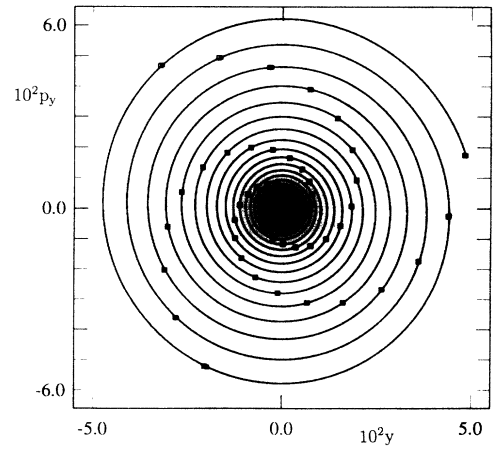

FIG. 5. Projection of the spiral invariant curve from a complex unstable periodic orbit (with $\theta \approx 2\pi/3$). The analytically obtained points (open squares) are compared with the numerical calculated points (filled squares), which, in most of the cases, coincide.

$$\xi(0)=c_1\mathbf{x}_0+c_2\mathbf{y}_0+c_3\mathbf{u}_0+c_4\mathbf{w}_0 ,$$

after n periods, gives

$$\begin{aligned}\xi(nT)=e^{n\lambda T}\{&[c_1\cos(n\theta)+c_2\sin(n\theta)]\mathbf{x}_0\\&+[c_2\cos(n\theta)-c_1\sin(n\theta)]\mathbf{y}_0\}\\+e^{-n\lambda T}\{&[c_3\cos(n\theta)+c_4\sin(n\theta)]\mathbf{u}_0\\&+[c_4\cos(n\theta)-c_3\sin(n\theta)]\mathbf{w}_0\} .\end{aligned}\tag{A5}$$

If we take $c_1=1$ and $c_2=c_3=c_4=0$ we find that the projections of $\xi(nT)$ along the axes $i=1,2$ are

$$\xi_1(nT)=e^{n\lambda T}[\cos(n\theta)\mathbf{x}_{01}-\sin(n\theta)\mathbf{y}_{01}] ,\tag{A6}$$

$$\xi_2(nT)=e^{n\lambda T}[\cos(n\theta)\mathbf{x}_{02}-\sin(n\theta)\mathbf{y}_{02}] .\tag{A7}$$

Eliminating $n\theta$ from Eqs. (A6) and (A7) we find

$$\begin{aligned}e^{2n\lambda T}(x_{02}y_{01}-x_{01}y_{02})^2=&(x_{01}\xi_2-x_{02}\xi_1)^2\\&+(y_{01}\xi_2-y_{02}\xi_1)^2 .\end{aligned}\tag{A8}$$

This equation is of the form

$$\alpha_1\xi_1^2+\beta_1\xi_1\xi_2+\gamma_1\xi_2^2=-\delta e^{2n\lambda T} ,\tag{A9}$$

with $\alpha_1>0$, $\gamma_1>0$, and $\delta<0$. Thus, the successive points with $n=1,2,\ldots,$ spiral outwards on the plane (ξ_1,ξ_2).

An example is shown in Fig. 5 where the projection of a spiral curve on the (y,p_y) plane is compared with the numerically computed points. In a similar way an orbit with $c_3=1$ and $c_1=c_2=c_4=0$ spirals inwards.

[1] M. C. Gutzwiller, in *Chaos in Classical and Quantum Mechanics* (Springer-Verlag, New York, 1990), Vol. 1.
[2] M. C. Gutzwiller, J. Math. Phys. **8**, 1979 (1967).
[3] M. C. Gutzwiller, J. Math. Phys. **12**, 343 (1971).
[4] R. Balian and C. Bloch, Ann. Phys. **85**, 514 (1974).
[5] M. V. Berry and M. Tabor, Proc. R. Soc. London Ser. A **356**, 373 (1977).
[6] W. H. Miller, J. Chem. Phys. **63**, 996 (1975).
[7] S. W. McDonald and A. N. Kaufman, Phys. Rev. Lett. **42**, 1189 (1979).
[8] E. J. Heller, Phys. Rev. Lett. **53**, 1515 (1984).
[9] H. Friedrich and D. Wintgen, Phys. Rep. **183**, 37 (1989).
[10] J. Guckenheimer and P. Holmes, *Nonlinear Oscillations, Dynamical Systems, and Bifurcations of Vector Fields* (Springer-Verlag, New York, 1983).
[11] R. A. Broucke, NASA Technical Report No. 32-1360, 1969 (unpublished).
[12] M. Founargiotakis, S. C. Farantos, G. Contopoulos, and C. Polymilis, J. Chem. Phys. **91**, 1389 (1989).
[13] G. Contopoulos and P. Magnenat, Cel. Mech. **37**, 387 (1985).
[14] G. Contopoulos, Cel. Mech. **38**, 1 (1986).
[15] D. Kosloff and R. Kosloff, J. Comput. Phys. **52**, 35 (1983).
[16] M. Baranger, Phys. Rev. **111**, 481 (1958).
[17] E. J. Heller and M. J. Davis, J. Phys. Chem. **84**, 1999 (1980).
[18] J. M. Gomez Llorente and H. S. Taylor, J. Chem. Phys. **91**, 953 (1989).
[19] E. J. Heller, Phys. Today **46**, (7), 38 (1993).
[20] S. C. Farantos and M. Founargiotakis, Chem. Phys. **142**, 345 (1990).
[21] R. Prosmiti and S. C. Farantos (unpublished).